RESEARCH PAPER

Characteristics and Synthesis of TiO$_2$ and B-TiO$_2$ by Solvothermal Method

Enas Mohamed Taha *, Nadia A. Abdulrahman*

Department of Chemistry, College of Science, University of Baghdad, Baghdad, Iraq

ARTICLE INFO

ABSTRACT

Titanium dioxide was prepared under high temperature and pressure by solvothermal method. XRD crystallography of TiO$_2$ showed decreases in crystalline size with increasing temperature, which means an increase in the surface area that increases the activity of the compound. Whereas in B-TiO$_2$, the crystal size decreased to and then increased again at, and it was a doping of 5% by weight of boric acid. We used temperatures of 70, 100, 130, 160 and 190 °C, respectively, and the energy gap values in the pure state were 3.23, 3.21, 3.11, 3.04 and 3.01 eV, respectively, while the energy gap values for B-TiO$_2$ were 2.94, 2.5, 2.7, 2.4 and 3.04 eV, respectively. XRD measurements were taken at three temperatures of 70, 130 and 190, respectively. The crystal thickness according to XRD measurements for pure substance was 29.1, 7.61, and 1.046 nanometers, respectively, while crystal thickness for B-TiO$_2$ was 15.575, 6.887, and 9.79 nanometers, respectively. FE-SEM measurements were taken at three temperatures of 70, 130, and 190, respectively. The diameters of the crystals according to FE-SEM measurements for TiO$_2$ were 19.245, 24.00286, and 25.21 nanometers, respectively, while the crystal diameters for B-TiO$_2$ were 13.68, 60.68714 and 57.00714 nanometers, respectively. The shapes of nanoparticles ranged between nanorods, nanotubes, and nanoflowers. We expect these structures to have promising future features in various applications.

INTRODUCTION

Nanotechnology is commonly used by emerging technologies. Nanoparticle are small particles with average diameters of less than 100 nanometers. As the size of these materials approache the nanoscale, their properties alter. When compared to bulk materials, nanoparticles feature show a number of unique qualities. One of the most essential properties of these nanoparticles is their ability to recognize steric stabilization, which leads to an increase in particle stability in biological systems. This opens up the possibility of employing nanoparticles in drug delivery systems (DDS)[1,2]. TiO$_2$ has been extensively explored as a popular n-type semiconductor photocatalyst due to its chemical, thermal, nontoxic properties as well as its inexpensive cost [3]. However, because of huge band gap values and high recombination rate of photogenerated charge carriers, it has low photocatalytic efficiency; which limits its large-scale uses in photocatalysis[4,5]. To improve photocatalytic activity, producing

* *Corresponding Author Email: inas.taha1205@sc.uobaghdad.edu.iq*

and developing doped TiO$_2$ materials to promote charge separation efficiency and improve light absorption has been recommended. To improve the photocatalytic efficiency of TiO$_2$, numerous modification procedures have recently been used, such as doping with ions (Cu, Ni, B) [6,7,8]. In order to ensure effective electron extraction and thus balanced carrier transport, the optimal state in TiO$_2$ electron transport layer it is used should have a high electron concentration as well as a high electron mobility; this according to the theoretical model of electrical conductivity.

Boron (B) doping has previously been shown to increase electron injection from excited dye molecules to the TiO$_2$ photo anode, resulting in improved dye-sensitized solar cell power conversion efficiency. It was recently found that a small amount of boron doping could improve TiO2 carrier mobility and electrical conductivity [9]. As a result, B-doped TiO$_2$ (abbreviated as B-TiO$_2$) is known to be a suitable electron transport layer for Perovskite solar cells in order to concurrently improve power conversion efficiency and reduce hysteresis [10]. Due to high pressure/temperature inside the closed environment of the autoclave, solvothermal approach is a relatively simple and straightforward way to modify the morphology of nanoparticles [11-15]. Through our research, we expect to reduce the energy gap of titanium dioxide as well as improve the photoelectric and optical properties through boron doping in a simple and inexpensive way.

MATERIALS AND METHODS

Titanium oxide nanoparticles were synthesized by modified solvothermal methodat at different temperatures of The solution was prepared by adding 500mg TiO$_2$ bulk (99%, M.Wt=79.87g/mol, HIMEDIA) into 50 ml of 10 M sodium hydroxid (NaOH, M.Wt.=40 g/mol, 98%, ALPHA) aqueous solution. The suspension system was stirred for 1hour at room temperature to form a homogeneous solution. When doping with Boric acid () in the ratio of 5 wt%, the same method was used with addition of 25 mg of boric acid. Then, the mixture was transferred to the autoclave was lined with Teflon and then well-sealed with a stainless steel top with a stainless steel temperature probe. A thermocouple is put in a heating coil attached to a temperature regulating board in this probe. The autoclave was heated for 10 hours at temperatures of 70,100,130,160, and 190 °C (heating rate=4°C/min). The cell was then cooled in air to reach the room temperature. The solution was separated by centrifuge with a speed of 4000 rpm for 10 to 15 min, and then, the precipitates were collected. The collected powders (white to pale yellow and light gray) were washed with deionized water, filtered and washed repeatedly until reached the pH of (6.8-7.2). The products were then immersed
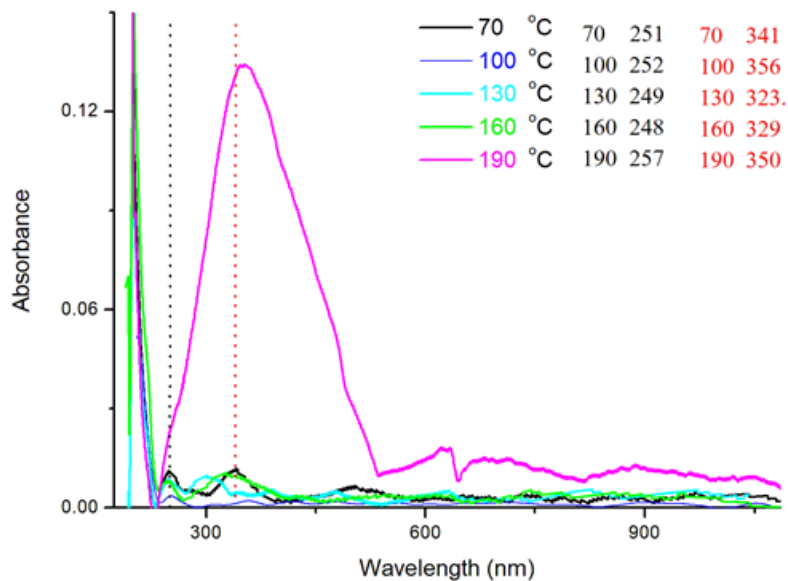
Fig. 1. UV spectra for TiO$_2$ nanoparticles at different temperatures of (70-190) °C at the region of (170-1080) nm.

in 300 ml of 0.1M Hydrochloric acid (HCl, 35.4%, M.Wt=36.46g/mol,CDH) solution for one hour, followed by filtering and repeatedly washed by deionized water until reached the pH of (6.8-7.2). The washed samples were dried in oven at 80 °C for 24 hours. Finally, the powders were sintered in furnace for 4 hours at 400 °C. All samples were saved in a storage.

RESULTS AND DISCUSSION

UV-vis measurements

UV-vis measurements gave us an idea about the size of the particles, as well as the energy gap values, and thus gave us a preliminary idea of the optical and photoelectric properties of these materials.

According to Tauc plot: $(\alpha h v)^n = K(h v - E_g)$

In this equation, α is the absorption coefficient, $h v$ is incident photon energy, K is energy independent constant, and E_g is the optical band gap energy of nanomaterials, the exponent n indicates the essence of a transition [16].

At 70 ℃, the value of energy gap for was 3.23 eV, while the value of energy gap for was 2.94 eV. We noticed a clear decrease in the value of the energy gap in the presence of boron for the same temperatures. While at temperature of 100 ℃, the energy gap was 3.21 eV for , and 2.50 eV for ·Again, we noticed a clear decrease in the value of the energy gap in the presence of boron for the
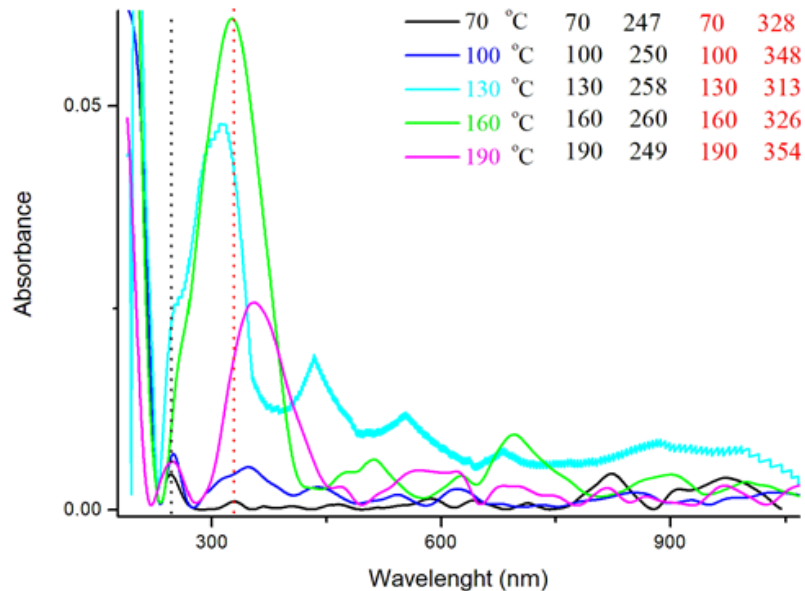
Fig. 2. UV spectra for B-TiO₂ nanoparticles at different temperatures of (70-190) ℃ at the region of (170-1080) nm.

Table 1. Energy gab values for TiO₂ and B- TiO₂ nanoparticles prepared at 70, 100, 130, 160 and 190 °C and calculated via Tauc plot extrapolation methods.

Temperature (℃)	TiO₂	B- TiO₂
	Energy gap/eV	Energy gap/eV
70	3.23	2.94
100	3.21	2.5
130	3.11	2.7
160	3.04	2.4
190	3.01	3.04

same temperature, and the value of the decrease depends on the type of doping. At 130 °C the value of energy gap for was 3.11 eV, while the value of energy gap for was 2.70 eV. At temperature of 160 °C, the value of energy gap was 3.04 eV for , and the value of energy gap was 2.40 eV for . Finally, at temperature of 190 °C, the value of energy gap was 3.01 eV for , while the value of energy gap was 3.04 eV for .. In general, the arising order of the energy gap values was We believe the reason for the apparent discrepancy in the energy gap values for B-TiO$_2$ is due to several reasons: first, the metal oxides that have been doped with have energy gap values that are much lower than the energy gap value for titanium dioxide, therefore, the energy gap value is expected to decrease and the value of the decrease depends on the type of doped metal and the percentage of doping, secondly, one of the most important influencing factors

is the metallurgy of each material or the crystal structure of the material, which depends mainly on temperature and pressure formation, as well as heating speed and cooling speed.

XRD Crystallography

XRD crystallography gave us a lot of information about the nature of crystals, the most important of which are crystal size and shape, as well as distortions that may occur in the crystal structure.

From XRD pattern of B-TiO$_2$ in Fig. 5, we noticed a large convergence at 70 °C with pure titanium dioxide at same temperature as shown in Fig. 4 i.e. convergence in values of angles unit shoulders. This means that at low temperature, doping by boron with such a large difference percent not occur on the crystal shape or size, and through Scherrer equation calculations, it was found that the crystal thickness at 70 °C is equal to 15.575
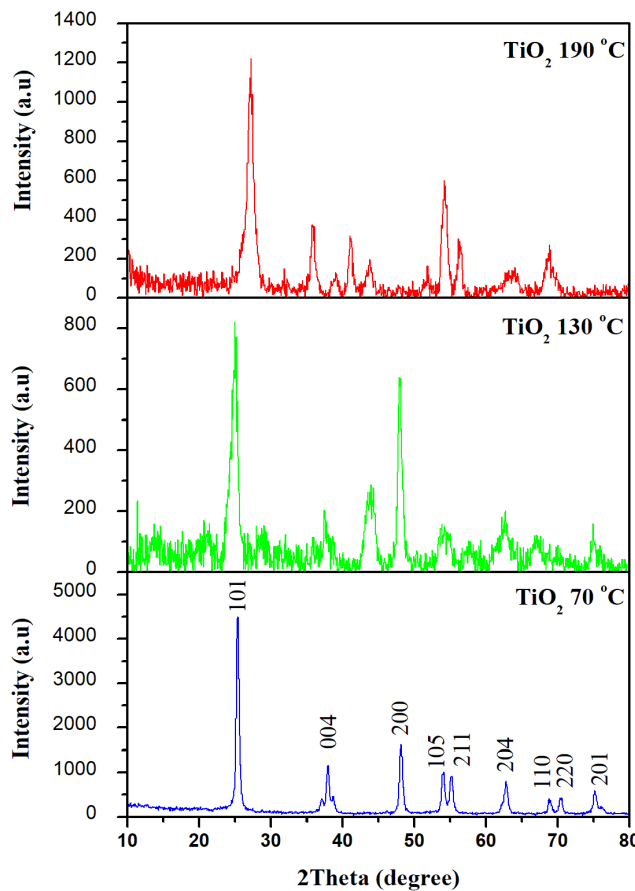
Fig. 3. XRD crystallography for TiO$_2$ nanoparticles at temperatures of 70, 130 and 190. JCPDS card no. 21-1272

nm, which means less than the thickness of the prepared crystals are at the same temperature in the pure state as shown in Table 2.

As increasing temperature and when it reaches 130 °C, we noticed an increase in the values of the angles and a small change in the positions with an increase in width of the shoulders and a large decrease in the absorbance. This means a significant decrease in the crystal size, which could be reflected on the optical properties of TiO$_2$ as a semiconductor. The size of crystals reached 6.887nm, which means smaller than the thickness of the crystals prepared at the same temperature at the pure state, see Table 2.At temperature of
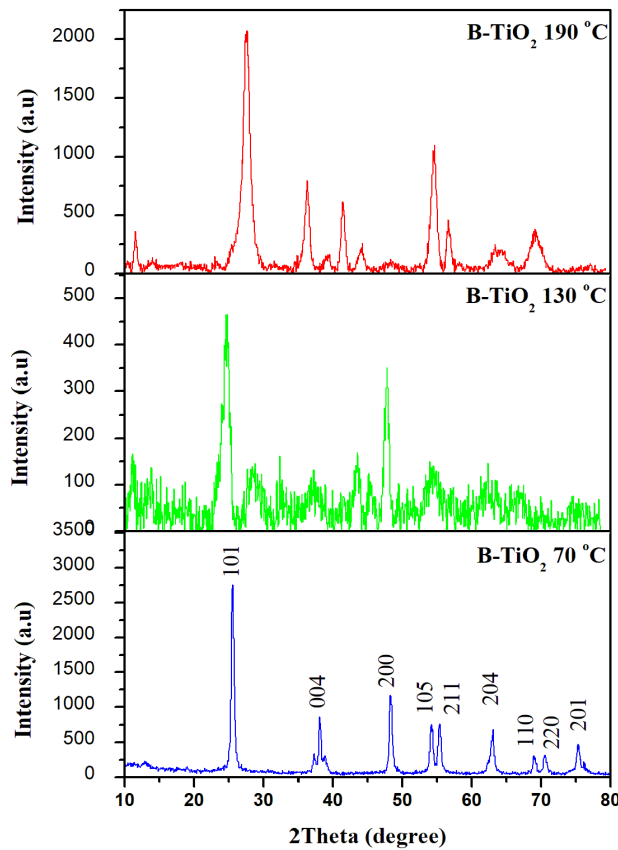
Fig. 4. XRD crystallography for B-TiO$_2$ nanoparticles at temperatures of 70, 130 and 190. JCPDS card no. 21-1272

Table 1. Energy gab values for TiO$_2$ and B- TiO$_2$ nanoparticles prepared at 70, 100, 130, 160 and 190 °C and calculated via Tauc plot extrapolation methods.

Substance	Temperatures °C	Å	D (nm)
	70	291	29.1
TiO$_2$	130	76.1	7.61
	190	10.4	1.04
	70	155.7	15.57
B-TiO$_2$	130	68.87	6.88
	190	97.9	9.79

190 ℃, it is noticed that the shoulders are sharper and the intensities are higher than 130 °C, which means that the crystals sizes increased, but it remains less than those prepared at 70 ℃. When compared with the same temperature in the pure state, the intensities are more intense and the shoulders are sharper. This gives an idea that the crystal size is larger. From Scherrer equation, the thickness of B-TiO$_2$ crystals at 190 ℃ equals 9.79nm, which is greater than those prepared at

130 ℃ andat190 ℃ in the pure state[17,18]. , see Table 2.

Field Emission Scanning Electron Microscopes (FE-SEM)

The importance of FE-SEM images is to display three-dimensional images of the samples, and this gives us an idea of the shape and dimensions of the nanoparticles.

From Fig. 6, we noticed that at temperature
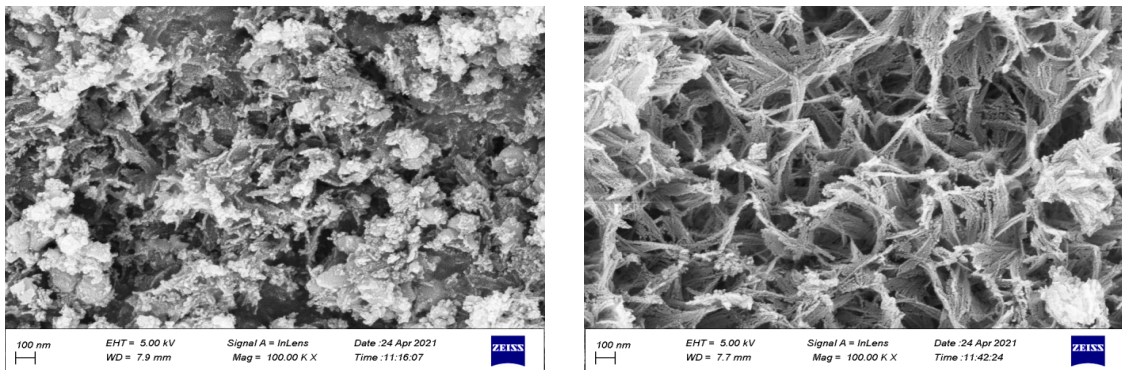
Fig. 5. FE-SEM images for a. TiO$_2$ nanoparticles and b. B-TiO$_2$ nanoparticles. Both samples were prepared at .
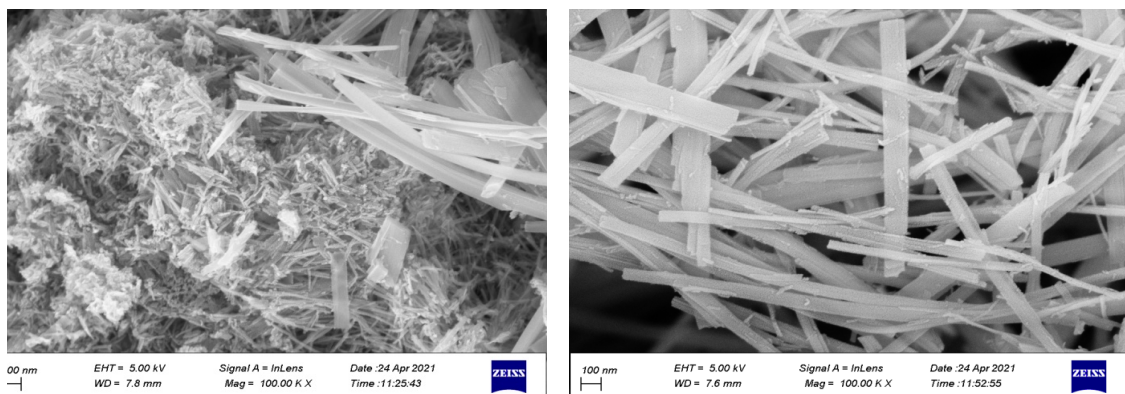
Fig. 6. FE-SEM images for a.TiO$_2$ nanoparticles and b. B-TiO$_2$ nanoparticles. Both samples were prepared at.

Table 3. The increase in dimensions as temperatures increase for TiO$_2$ and B-TiO$_2$ nanoparticles by FE-SEM image.

Substance	Temperatures (℃)	Average Diameters (nm)
	70	19.24
TiO$_2$	130	24.00
	190	25.21
	70	13.68
B-TiO$_2$	130	60.68
	190	57.00

of the sizes of the nanoparticles of B-TiO$_2$ are smaller than the sizes of the pure state, as shown in the table 3, and the shapes of the particles are a nanodots for both of them.

From Fig. 7, we noticed that at temperature of the size of the nanoparticles of B-TiO$_2$ are bigger than the sizes of the pure state, as shown in the table 3, and the shape of the particles are nanorods for both of them.

While from Figure 8, we noticed that at temperature of the size of the nanoparticles of B-TiO$_2$ are bigger than the sizes of the pure state, as shown in the table 3, and the shapes of TiO$_2$ particles are nanorods and B-TiO$_2$ are nano flowers and nanotubes.

According to Table 3, the highest particulate thickness was recorded at for B-TiO$_2$, while the lowest nanoparticles size was recorded at in B-TiO$_2$, But the order of the sizes was generally from top to bottom B-TiO$_2$>TiO$_2$ [19].

CONCLUSION

The properties of titanium dioxide were found to be improved with increasing temperature the energy gap values increased as the size decreases, which means an increase in the surface area. Also, the crystal size decreases in the presence of boron, and the shape of the nanoparticle's changes depending on temperature, pressure, type and percentage of doping and the period for manufacturing. We cannot say which sample is better because it depends on the need of the users and the applications.

CONFLICT OF INTEREST

The authors declare that there is no conflict of interests regarding the publication of this manuscript.

REFERENCES

1. Mahmoodi NO, Ghavidast A, Amirmahani N. A comparative study on the nanoparticles for improved drug delivery systems. Journal of Photochemistry and Photobiology B: Biology. 2016;162:681-693.
2. Çeşmeli S, Biray Avci C. Application of titanium dioxide (TiO$_2$) nanoparticles in cancer therapies. J Drug Target. 2018;27(7):762-766.
3. Liu G, Hoivik N, Wang K, Jakobsen H. Engineering TiO2 nanomaterials for CO$_2$ conversion/solar fuels. Sol Energy Mater Sol Cells. 2012;105:53-68.
4. Li H, Duan X, Liu G, Liu X. Photochemical synthesis and characterization of Ag/TiO$_2$ nanotube composites. JMatS. 2008;43(5):1669-1676.
5. Ismael M. Enhanced photocatalytic hydrogen production and degradation of organic pollutants from Fe (III) doped TiO$_2$ nanoparticles. Journal of Environmental Chemical Engineering. 2020;8(2):103676.
6. Pandiyaraj KN, Vasu D, Ghobeira R, Tabaei PSE, De Geyter N, Morent R, et al. Dye wastewater degradation by the synergetic effect of an atmospheric pressure plasma treatment and the photocatalytic activity of plasma-functionalized Cu-TiO$_2$ nanoparticles. J Hazard Mater. 2021;405:124264.
7. Barkul RP, Sutar RS, Patil MK, Delekar SD. Photocatalytic Degradation of Organic Pollutants by Using Nanocrystalline Boron-doped TiO$_2$ Catalysts. ChemistrySelect. 2021;6(14):3360-3369.
8. Gomez-Solis C, Mendoza R, Rios-Orihuela JF, Robledo-Trujillo G, Diaz-Torres LA, Oliva J, Rodriguez-Gonzalez V. Efficient solar removal of acetaminophen contaminant from water using flexible graphene composites functionalized with Ni@TiO$_2$:W nanoparticles. J Environ Manage. 2021;290:112665.
9. Tian H, Xin F, Tan X, Han W. High lithium electroactivity of boron-doped hierarchical rutile submicrosphere TiO$_2$. J Mater Chem A. 2014;2(27):10599-10606.
10. Shi X, Ding Y, Zhou S, Zhang B, Cai M, Yao J, et al. Enhanced Interfacial Binding and Electron Extraction Using Boron-Doped TiO$_2$ for Highly Efficient Hysteresis-Free Perovskite Solar Cells. Advanced science (Weinheim, Baden-Wurttemberg, Germany). 2019;6(21):1901213-1901213.
11. Parveen S, Paul KK, Giri PK. Precise Tuning of the Thickness and Optical Properties of Highly Stable 2D Organometal Halide Perovskite Nanosheets through a Solvothermal Process and Their Applications as a White LED and a Fast Photodetector. ACS Applied Materials & Interfaces. 2020;12(5):6283-6297.
12. Ramesh Gadhave Jayshree S. Degradation of Dyes by Implementation of Biogenically Synthesized Zinc Oxide. International Journal of Science and Research (IJSR). 2023;12(7):663-667.
13. Abdulrahman NA. Braggs, Scherre, Williamson–Hall and SSP Analyses to Estimate the Variation of Crystallites Sizes and Lattice Constants for ZnO Nanoparticles Synthesized at different Temperatures. Neuroquantology. 2020;18(1):53-63.
14. Saif TA, Nadia AA. Cu-ZnO Nanostructures Synthesis and Characterization. Iraqi Journal of Science. 2021:708-717.
15. Lee S, Hu Y. Preparation and characterization of La$_{0.5}$Sr$_{0.5}$CoO$_3$/Al-doped ZnO thin film heterojunctions. Solid State Communications. 2012;152(2):81-84.
16. Makuła P, Pacia M, Macyk W. How To Correctly Determine the Band Gap Energy of Modified Semiconductor Photocatalysts Based on UV–Vis Spectra. The Journal of Physical Chemistry Letters. 2018;9(23):6814-6817.
17. Salman ON, Agool IR, Ismail MM. Preparation of the scattering layer based on TiO2 nanotube and their dye sensitized solar cell applications. Appl Phys A. 2017;123(6).
18. Ho C-Y, Lin JK, Wang H-W. Characteristics of Boron Decorated TiO$_2$ Nanoparticles for Dye-Sensitized Solar Cell Photoanode. International Journal of Photoenergy. 2015;2015:1-8.
19. Gupta T, Samriti, Cho J, Prakash J. Hydrothermal synthesis of TiO2 nanorods: formation chemistry, growth mechanism, and tailoring of surface properties for photocatalytic activities. Materials Today Chemistry. 2021;20:100428.